



# Measuring the spatiotemporal variability in snow depth in subarctic environments using UASs – Part 2: Snow processes and snow–canopy interactions

Leo-Juhani Meriö<sup>1,2</sup>, Anssi Rauhala<sup>3</sup>, Pertti Ala-aho<sup>1</sup>, Anton Kuzmin<sup>4</sup>, Pasi Korpelainen<sup>4</sup>, Timo Kumpula<sup>4</sup>, Bjørn Kløve<sup>1</sup>, and Hannu Marttila<sup>1</sup>

<sup>1</sup>Water, Energy and Environmental Engineering, Faculty of Technology, University of Oulu, Oulu, 90014, Finland

<sup>2</sup>Water Resources, Finnish Environment Institute (Syke), 90014, Oulu, Finland

<sup>3</sup>Civil Engineering, Faculty of Technology, University of Oulu, Oulu, 90014, Finland

<sup>4</sup>Department of Geographical and Historical Studies, University of Eastern Finland, Joensuu, 80101, Finland

**Correspondence:** Leo-Juhani Meriö (leo-juhani.merio@syke.fi)

Received: 1 December 2022 – Discussion started: 2 January 2023

Revised: 16 June 2023 – Accepted: 17 August 2023 – Published: 17 October 2023

**Abstract.** Detailed information on seasonal snow cover and depth is essential to the understanding of snow processes, to operational forecasting, and as input for hydrological models. Recent advances in uncrewed or unmanned aircraft systems (UASs) and structure from motion (SfM) techniques have enabled low-cost monitoring of spatial snow depth distribution in resolutions of up to a few centimeters. Here, we study the spatiotemporal variability in snow depth and interactions between snow and vegetation in different subarctic landscapes consisting of a mosaic of conifer forest, mixed forest, transitional woodland/shrub, and peatland areas. To determine the spatiotemporal variability in snow depth, we used high-resolution (50 cm) snow depth maps generated from repeated UAS–SfM surveys in the winter of 2018/2019 and a snow-free bare-ground survey after snowmelt. Due to poor subcanopy penetration with the UAS–SfM method, tree masks were utilized to remove canopy areas and the area (36 cm) immediately next to the canopy before analysis. Snow depth maps were compared to the in situ snow course and a single-point continuous ultrasonic snow depth measurement. Based on the results, the difference between the UAS–SfM survey median snow depth and single-point measurement increased for all land cover types during the snow season, from +5 cm at the beginning of the accumulation to –16 cm in coniferous forests and –32 cm in peatland during the melt period. This highlights the poor representation of point measurements in selected locations even on the

subcatchment scale. The high-resolution snow depth maps agreed well with the snow course measurement, but the spatial extent and resolution of maps were substantially higher. The snow depth range (5th–95th percentiles) within different land cover types increased from 17 to 42 cm in peatlands and from 33 to 49 cm in the coniferous forest from the beginning of the snow accumulation to the melt period. Both the median snow depth and its range were found to increase with canopy density; this increase was greatest in the conifer forest area, followed by mixed forest, transitional woodland/shrub, and open peatlands. Using the high-spatial-resolution data, we found a systematic increase (2–20 cm) and then a decline in snow depth near the canopy with increasing distance (from 1 to 2.5 m) of the peak value through the snow season. This study highlights the applicability of the UAS–SfM in high-resolution monitoring of snow depth in multiple land cover types and snow–vegetation interactions in subarctic and remote areas where field data are not available or where the available data are collected using classic point measurements or snow courses.

## 1 Introduction

Snow cover is of great importance for northern ecosystems and hydrology, providing shelter for plants and animals in the harsh winter conditions and maintaining freshwater re-

sources and seasonal hydrological processes (Pomeroy and Brun, 2001; Mankin et al., 2015; Blume-Werry et al., 2016). The water that is stored in the snowpack during the winter is released in spring freshet, recharging groundwater and soil water and ultimately maintaining low-flow conditions in early summer (Earman et al., 2006; Godsey et al., 2014; Meriö et al., 2018). Additionally, snow conditions are essential for several ecosystem services, including recreational and tourism uses (Scott et al., 2008; Neuvonen et al., 2015). Numerous studies have documented the changes and their regional variability in snow conditions in Finland (Luomaranta et al., 2019) and the Northern Hemisphere (Brown and Robinson, 2011; Pulliainen et al., 2020). The ongoing environmental change and future projections involve snow conditions that are changing rapidly in high-latitude regions (Musselman et al., 2017; Mudryk et al., 2020). Snow processes are known to have high spatiotemporal variability, thus more detailed high-resolution knowledge of snow accumulation and melt is needed to support process understanding, modeling, forecasting, and decision-making.

The spatiotemporal variability in snow accumulation is governed by climate, terrain characteristics, and vegetation cover at scales above 100 m and by wind redistribution, microtopography, and canopy interception at scales below 100 m (McKay and Gray, 2004). However, in nature the distinct limits for factors controlling snow depth at different spatial scales are varying. Forested and open areas have different snow accumulation and melt characteristics (Pomeroy et al., 2002; Gelfan et al., 2004). In forests, the snow depth has been found to depend on canopy cover with less snow in the denser forest because of canopy interception and sublimation (Varhola et al., 2010). In forest openings, the snow depth depends, among other things, on their size, with most snow accumulating in clearings 2–5 times the height of nearby trees (Pomeroy et al., 2002). In larger open areas, wind erosion and drift redistribute the snow to the sheltered forest edges where the wind speeds are reduced (Hiemstra et al., 2002). Snowmelt is governed by the energy available for melt, mainly influenced by topography and vegetation (Jost et al., 2007). Generally, snow melt rates are lower in shadowed areas, like topographic depressions, northern slopes, and areas shaded by dense forest canopies (Gary, 1974; Clark et al., 2011). However, longwave radiation from forest canopies can also increase the melting speed near the trees (Golding and Swanson, 1978). Additionally, the timing of snow depletion is dependent on the amount of pre-melt snow (Liston, 1999; Faria et al., 2000).

Currently, there are various techniques to monitor snow properties, such as snow cover, depth, and snow water equivalent (Kinar and Pomeroy, 2015). Snow courses and measurement networks are established to improve the poor representation given by single-point measurements, but small-scale or even regional spatial variability is not captured using these techniques. Satellite remote sensing products extend the measurements to a large scale (Dietz et al., 2012), but the

resolution of the mature products is coarse ( $\sim 25$  km). Methods for higher-resolution satellite products are continuously under development. For example, Lievens et al. (2019) showcased a method for 1 km resolution snow depth retrieval for mountain regions. Airborne lidar from crewed aircraft provides high-resolution snow depth for relatively large areas but with high cost (Deems and Painter, 2006; Deems et al., 2013). The recently popularized uncrewed or unmanned aircraft systems (UASs), together with structure from motion (SfM) techniques, have shown the potential for cost-efficient solutions for high-resolution snow depth mapping (see accompanying article Part 1, Rauhala et al., 2023; Vander Jagt et al., 2015) enabling new methods of snow process research.

Previous UAS–SfM studies have focused on testing the accuracy of the method on mountainous regions or snow on tundra, glaciers, prairies, and meadows, with mostly low (grassland, shrub, bushes) or non-vegetated surfaces. A more comprehensive review of UAS–SfM studies is included in the accompanying paper (Rauhala et al., 2023). Snow process observations in UAS–SfM studies have mostly been related to topographic features such as aspect, cornices, gullies, exposed ridgelines, and broad elevated slopes (Bühler et al., 2016; Redpath et al., 2018; Niedzielski et al., 2019), as well as wind redistribution, snow erosion, and tree wells (Harder et al., 2020). Lenzioch et al. (2016) evaluated snow depth in an open and small forested area in Šumava National Park, Czech Republic, and found the accuracy was better in open areas than forested areas due to deadwood on the ground and vegetation effects. Niedzielski et al. (2019) observed snow depths in sites covering forests, meadows, and arable land in Poland, but these forested areas were removed as outliers from the snow depth maps. Subcanopy penetration of UAS–SfM was compared to UAS–lidar in subalpine areas and prairies in Canada with the conclusion that UAS–SfM is not capable of observing snow depth below the canopy (Harder et al., 2020). Most recently, Schirmer and Pomeroy (2020) studied the association between snow depth differences during the ablation period and snow cover brightness, slope, and initial snow depth at an alpine ridge in the Canadian Rocky Mountains. The previous studies have shown technical advancements and improved accuracies of UAS–SfM in snow monitoring. However, to our knowledge, no studies extend the focus to the snow processes: accumulation, ablation, and interactions between vegetation and snow in the subarctic boreal region, consisting of a mosaic of forested and peatland areas with challenging climate factors, such as variable light conditions and very cold temperatures.

The overall aim of this study was to evaluate the variability in snow accumulation and melt in high spatial resolution using UAS–SfM. With these novel datasets, we studied interactions between snow cover and vegetation in different subarctic land cover types. We compared the acquired snow depth data with manual snow course measurements and assessed the spatial representativeness of a single-point snow depth measurement in relation to UAS–SfM-derived data.

The specific research questions were as follows: (1) how does spatiotemporal snow depth variability differ across forested and open mire landscapes and (2) can we attribute the landscape differences to snow–canopy interaction processes using high-spatial-resolution UAS–SfM snow depth surveys.

## 2 Study area

Three test sites, mire (14.41 ha; Fig. 1c), mixed (15.40 ha; Fig. 1d), and forest (15.87 ha; Fig. 1e), with varying land cover were selected at a snow course transect in Lompolonjänkä catchment (68.00° N, 24.21° E) (Marttila et al., 2021), adjacent to Pallas-Yllästunturi National Park in the subarctic region (Fig. 1). The land cover in the catchment consists mostly of boreal coniferous forests and open peatlands. The most common tree species are Norway spruce (*Picea abies* (L.) H. Karst) with occasional Scots pine (*Pinus sylvestris* L.), downy birch (*Betula pubescens* Ehrh.), and mountain birch (*Betula pubescens* ssp. *czerepanovii*) (Sutinen et al., 2012). On open peatlands, as well as at times in the forested areas, there are occasional bushes and other low vegetation. The mire site consists mostly of flat open peatland, the forest site of gently sloping coniferous forest, and the mixed site of a relatively flat mixture of both. Elevation in the study area varies from 267 to 350 m a.s.l. (above sea level), the slope varies between 0–4.76° and the aspect is towards the west-northwest. Peatland areas, at the mire and mixed sites, are almost flat with a slope of 0–0.25°, while the slope is highest in parts of the forested area at the forest site.

Typically, stable snow cover in the area during 2006–2018 (the period of record) started building in mid-October, with peak accumulation (96 cm) at the beginning of April just before the melt season, with all snow having melted by the end of May (Fig. 2). During the study period, stable snow cover was established in late November, and the snow depth stayed significantly under its mean until the peak accumulation (100 cm on 23 March) when it slightly surpassed the long-term mean value. The melting period started rapidly due to a warm spell in early April, and all snow melted a few days earlier (26 May) than the average in the period of record 2006–2018. The mean annual temperature for the hydrological year (October–September) 2019 was 0.5 °C (0.4 °C in 2004–2018). Precipitation was 621 mm (638 mm in 2008–2018), which was made up of 40 % snowfall (42 % in 2008–2018). Snowfall was calculated from total precipitation using 1.1 °C as the threshold for snowfall (Feiccabrino and Lundberg, 2008; Jenicke et al., 2016). Open weather data from the Finnish Meteorological Institute (FMI) Kenttäröva measurement station were used for climate parameter calculations.

## 3 Materials and methods

### 3.1 UAS campaigns and reference measurements

Data from five of the seven UAS campaigns were selected for snow process analysis. Two of the surveys were discarded due to challenges that hindered the data collection. Camera mechanics froze due to very cold temperatures during the January survey, causing unfocused pictures. In May, only very small patches of snow, insufficient for the analysis, were remaining in study plots. During the snow period, the remaining surveys were conducted under varying snow, weather, and light conditions. They were held at the beginning (10–13 December 2018, DEC-12) and middle (18–22 February 2019, FEB-21) of the snow accumulation period, at the beginning of the melt period (1–5 April 2019, APR-03, shortly after peak accumulation), and in the middle of the melt period (22–25 April 2019, APR-24). The last survey (4–5 June 2019), for the snow-free conditions, was conducted before ground vegetation growth (when the vegetation was still compressed) approximately 1 week after all snow had melted.

The aerial surveys were done using four drones: DJI Phantom 4 RTK (real-time kinematic) quadcopter (P4RTK), DJI Mavic Pro, DJI Phantom 4, and eBee Plus RTK. We selected data from P4RTK because it provided the highest accuracy for snow and ground surface maps created using the SfM photogrammetry technique (see Rauhala et al., 2023). The flight height target was 110 m, which provided ~ 3 cm ground resolution. Forward and side overlap targets were at least 80 % and 75 %, respectively, for aerial pictures.

Before starting the aerial surveys, an average of 13 ground control points (GCPs) (8–17, median 14) and 16 random checkpoints (CPs) (6–38, median 15) were marked and measured using RTK GNSS (Global Navigation Satellite System) receivers (Trimble R10 and Topcon HiPer V) at each test plot during all campaigns. For the RTK-equipped drones, we selected the GCP that was nearest to the flight control for the snow/ground surface map calculations. All GCPs were needed when using data from non-RTK drones. CPs were used to estimate the accuracy of the snow and ground surface models.

During every UAS survey, reference snow depth was manually measured from a standardized snow course (46 stationary points with a mean distance of 50 m between points) transecting the study plots, with an accuracy of ±2 cm (see Rauhala et al., 2023, for details). In addition, data from an automatic ultrasonic snow depth sensor (Campbell Scientific SR50-45H) with an accuracy of ±1 cm, located in the forest plot at the highest elevation of the study area and operated by the FMI, were used as a reference to compare the UAS-derived snow maps. The Corine classification of Kenttäröva snow depth sensor location is coniferous forest, the distance to the canopies is approximately 5 m, and the understory in the sensor location is replaced with an artificial green grass

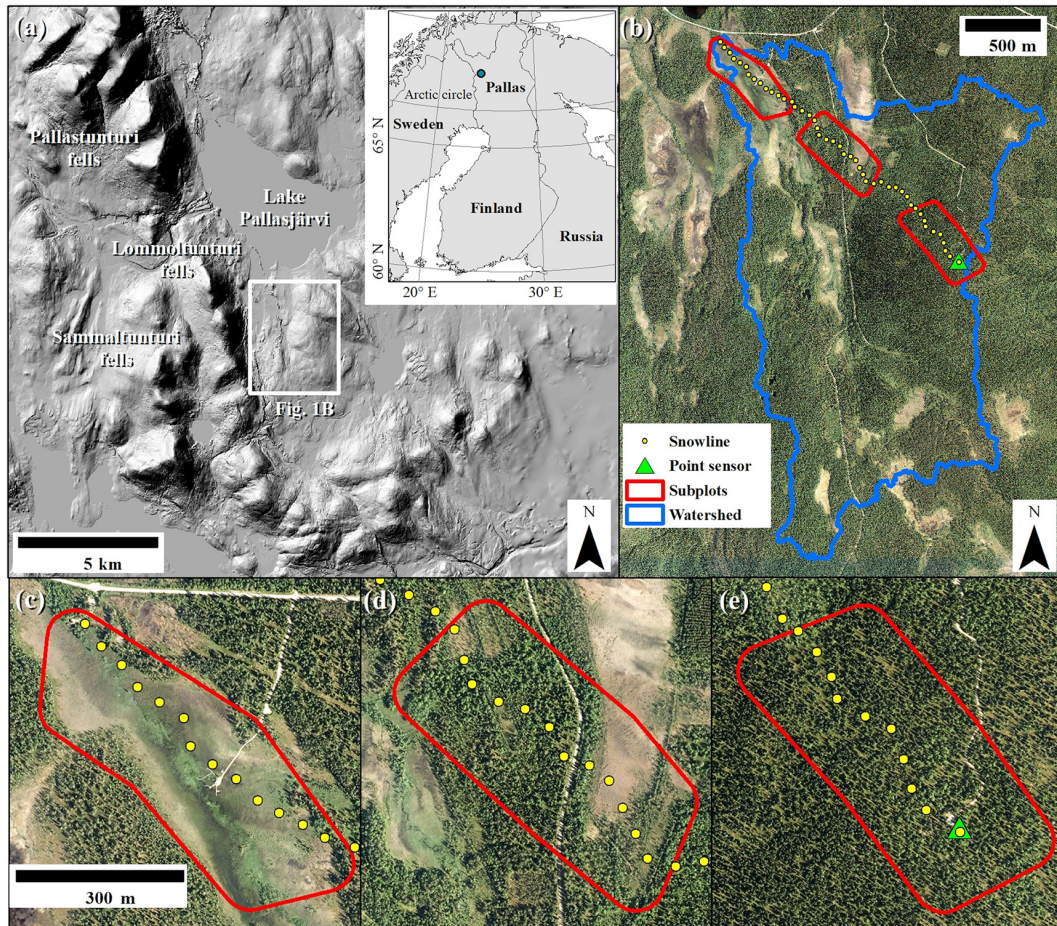


**Figure 1.** (a) The location of the study area south of Lake Pallasjärvi and east of the Lommoltunturi fells. The location of Fig. 1 (b) is highlighted by the white rectangle. Hillshade courtesy of the National Land Survey of Finland. (b) Locations of the manual snowline measurement, ultrasonic point sensor, and outlines of the subplots (sites mire, mixed, and forest read from northwest to southeast) within the catchment. Panels (c), (d), and (e) zoom in on the mire, mixed, and forest subplots, respectively. Orthophoto courtesy of the National Land Survey of Finland.

mat. More detailed information for the UAS campaigns and flight parameter selection can be found in the accompanying article (Rauhala et al., 2023).

### 3.2 High-resolution snow depth maps and tree mask

The principal technique for snow depth map generation was subtracting snow surface elevations from snow-free ground elevations. Agisoft PhotoScan/Metashape Professional v.1.4.5/v1.6.0 software (Agisoft, 2019) utilizing an SfM technique was used to create surface elevation maps using high-quality and moderate depth filtering settings (Agisoft, 2023). This resulted in full-resolution ( $\sim 3$  cm) orthomosaic and 2 times full-resolution snow and ground surface maps or digital surface models (DSMs). The processed data were exported as georeferenced files to ArcGIS 10.6 (Esri, 2019) for further processing.

Due to poor subcanopy penetration when using the UAS–SfM method (Harder et al., 2020), we omitted data at tree locations and immediately next to trees using special tree masks. Tree masks were generated using maximum likelihood supervised classification in ArcGIS 10.6 and full-resolution orthomosaics from the survey conducted on 3 April 2019. We selected this survey because snow had melted from the tree canopies, giving a clear contrast between trees and snow. This was then used for classifying the data. The SfM method had challenges in differentiating trees from snow cover from the data for surveys in which the canopies were covered by snow. This led to artificially increased snow depths next to the tree branches. Moreover, the deciduous trees without leaves were problematic in supervised classification because bare branches were easily mixed with shadowed snow cover, leading to the classification of shadowed snow cover as canopy or canopy as snow cover. To mitigate these methodical challenges, we tested different

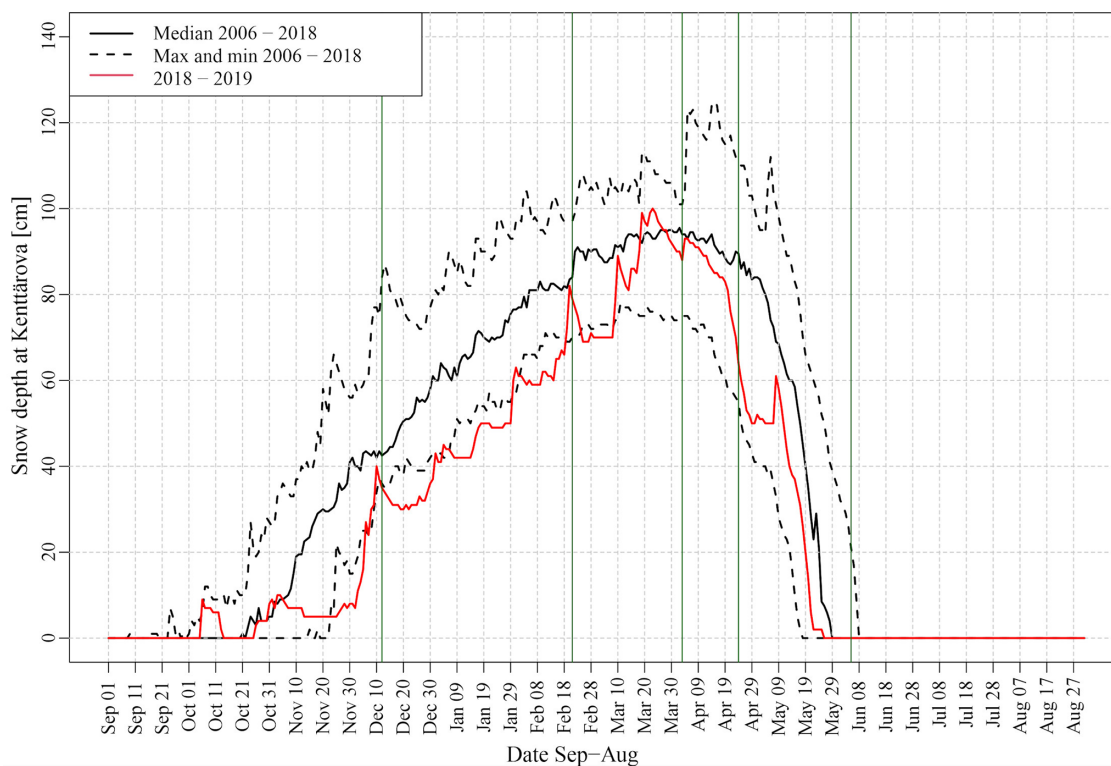


**Figure 2.** Typical snow conditions in the study area (Finnish Meteorological Institute (FMI) Kenttäröva point measurement) between 2006–2018 and during the study winter of 2018–2019 (in red). The min and max snow depth shows the minimum and maximum value for each date from all winters in the period of 2006–2018. Survey times are shown with vertical lines (dark green). Survey data from June 2018 were used to determine the ground digital elevation model.

buffer distances around the classified tree mask and found that 36 cm was a good trade-off for removing the compromised zones next to trees without losing too much valuable snow cover data. After buffering, the tree masks were saved at a resolution of 2 cm and applied to snow and ground surface maps before snow depth calculation.

Snow depths were calculated for each pixel by subtracting bare-ground (snow-free) elevation from snow surface elevation for each survey carried out in the snowy season, resulting in digital elevation maps (DEMs) of differences (DoDs). A DoD is used here interchangeably with snow depth map. Snow depth maps were aggregated to a 50 cm resolution before further data analysis. This resolution was chosen to smooth small-scale variability while keeping a reasonably high resolution for snow–vegetation interaction analysis. Moreover, the selected resolution followed findings from De Michele et al. (2016), where the standard deviation of snow depth increased with a decreased pixel size but stabilized for resolutions smaller than 1 m. For analyzing snow depth variability compared to point measurement, anomaly maps were created by subtracting the corresponding snow depth measured with ultrasonic sensors from each pixel of the UAS–SfM-derived snow depth maps. The snow depth calculated using ultrasonic sensors was also subtracted from

snow course measurements. The full workflow for tree mask and snow depth map generation, along with their calculated accuracy, is presented by Rauhala et al. (2023).

### 3.3 Land cover and snow processes

Corine land cover 2018 data with a resolution of 20 m (SYKE, 2019) were further used to study the snow processes for different land cover types: coniferous forest (10.07 ha), mixed forest (1.42 ha, made up of mixed (1.34 ha) and broad-leaved forest (0.08 ha) land cover types), transitional woodland/shrub (1.06 ha), and peat bogs (10.37 ha) (Fig. 3). The Corine land cover dataset (EEA, 2018) was selected for this purpose due to its (i) harmonized vegetation classification and (ii) availability across the Eurasian region, which readily enable expanding the future studies to larger regions and other areas. To further study the interactions between canopy cover and snow depth, the euclidian distance from the nearest tree mask pixel, representing the canopy, was calculated for each snow pixel in ArcMap 10.6 (Fig. 3). These distance masks were used to calculate median snow depth as a function of distance from the canopy for each land cover type.

Histograms, boxplots, statistical indicators (median, mean, and 5th–95th percentiles), and tests were used to study snow

depth variability and differences within and between different land cover types. The Kruskal–Wallis (K–W) test was selected to find whether there was a difference between group (land cover types) medians. To find which groups might differ, a Dunn's test (Dunn, 1964) with a Bonferroni adjustment (Dunn, 1961) was used. The large sample size (in total 917 045 snow pixels for each survey) caused problems in statistical analysis, as large sample sizes may be too big to fail (Lin et al., 2013). To mitigate the problem, we ran the Monte Carlo simulation by extracting 100 samples of sizes ranging from 100 to 4000, at an increment of 100, from each land-cover-type dataset and ran the K–W and Dunn's test for each sample to generate coefficient,  $p$  value, and sample size (CPS) charts.

## 4 Results

### 4.1 Spatiotemporal variability in snow depth during accumulation and melt

The snow depth anomaly in test sites compared to ultrasonic point measurements exposed high spatial variability in snow depth and differences from the point measurement (Fig. 4, Table 1). At the beginning of the snow accumulation (DEC-12), this difference was positive, showing slightly more snow (median +5 cm) in all sites compared to the single automated point measurement reference in the forest. In the middle of the snow accumulation season (FEB-21), however, the difference was slightly negative (median –3 cm). The negative difference increased (median –9 cm) at the beginning of melt (APR-03), reaching a peak during the middle of the melt period (APR-24), when a high negative difference (median –22 cm) was observed. This difference was highest in the mire site (median –28 cm) but was also present in the mixed site (median –24 cm), a partly covered open peat bog similar to the mire site, where the forest cover was more variable, including increased mixed forest and transitional woodland/scrub areas. In open peatlands, the snow had accumulated on the forested edges of the open areas. During the melt (APR-24), the forest site showed the smallest difference (median –8 cm) compared to the point measurement. The reference snow course measurements had similar snow depth central values and distribution compared to the UAS–SfM-derived snow depths (Fig. 5 and Tables 1, 2, and 3).

### 4.2 Land cover effect on snow depth variability

UAS–SfM-derived snow depths for DEC-12 were slightly higher compared to single-point measurement (median 5–6 cm) and similar for all Corine land cover types in the test area. The highest snow depth range was found in the mixed and coniferous forest (5%–95% range 35 and 33 cm, respectively), while in open peatlands and transitional woodland/shrub the range was lowest (5%–95% range 17 and 19 cm, respectively) (Fig. 5 and Tables 2 and 3). In the mid-

dle of the accumulation period, FEB-21, the snow depth was lower in open peatlands and transitional woodland/scrub (median –6 to –2 cm) than mixed and coniferous forests (median 1 cm) with a high range in forested areas (62–66 cm). For the beginning of the snowmelt period (APR-03), the median snow depths were lower compared to point measurement for all land cover types, with the highest negative difference in open peatlands (median –13 cm); for the other areas this difference was smaller (–6 to –5 cm). The spread of the snow depth was similar (32–35 cm) for all land covers. The biggest difference in variability between land cover types was observed in the middle of the melt period (APR-24). Again, the difference compared to the single-point reference was highest in open peatland (median –32 cm) followed by transitional woodland/shrub (–22 cm). In mixed and coniferous forests, the difference was lower (median –16 and –13 cm, respectively). The range of the snow depth was high for all land cover types (42–49 cm). The snow depth range increased throughout the snow season, except for in mixed and coniferous forest areas in FEB-21, when the range was at its highest in all the surveys (Table 3). The increase in snow depth variability can be clearly observed in Fig. 5, which shows the snow depth distributions and median snow depths for each survey time and land cover type. The distributions generally follow a normal distribution with increasing tail lengths towards the end of winter.

For the full dataset, the Kruskal–Wallis test showed significant ( $p < 0.001$ ) differences between land cover types for median snow depth in all surveys from DEC-12 to APR-24, with increasing chi-squared values: 3391, 86 489, 92 497, and 237 345, respectively. Dunn's post hoc test with a Bonferroni adjustment showed that all median snow depths between land cover types were different from each other for all surveys. The number of observations in the full dataset was 403 443, 56 426, 42 327, and 414 849 for the coniferous forest, mixed forest, transitional woodland/shrub, and peat bogs, respectively.

However, using the UAS–SfM method, the number of data points is very large, potentially making it difficult for the test to accept the null hypothesis (Lin et al., 2013). To address this, we reduced the sample size with random sampling to highlight the true differences between the land cover types. The CPS charts (see Figs. S1–S4 in the Supplement) show that with smaller random sample sizes the differences between snow depth medians are not that evident. For DEC-12, the CPS chart indicates how median snow depths are similar between all land cover types when the sample size is 100. With an increasing sample size, the similarity is still clearly visible for the pairs of peat bog and conifer forest and transitional woodland/shrub and mixed forest. For FEB-21, the differences in median snow depth increased, but even with a small sample size, the similarity is visible for the pairs of conifer forest and transitional woodland/shrub and transitional woodland/shrub and mixed forest. It remained similar for conifer forest and mixed forest with a larger sample sizes.

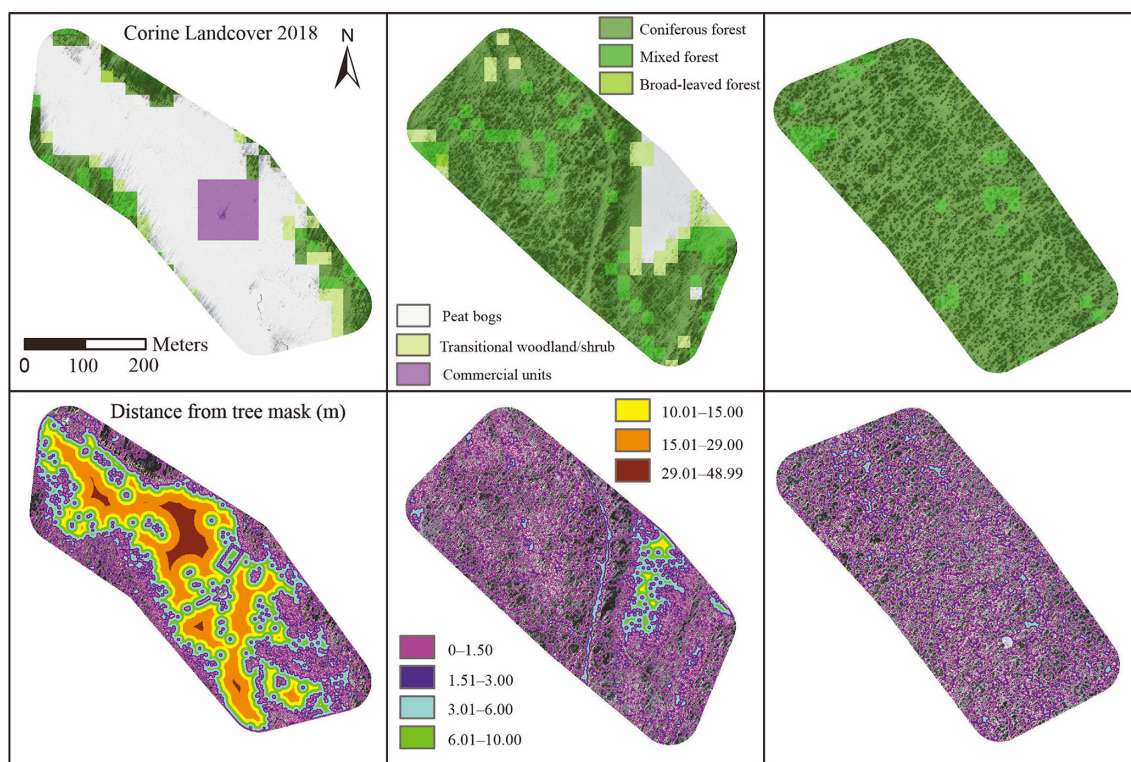


**Figure 3.** Corine land cover (2018) data (above) and distance from tree mask (below) (calculated using a euclidian distance tool in ArcMap 10.6) for test sites. “Commercial units” refers to measurement infrastructure in the peat bog.

**Table 1.** Median snow depths of the UAS–SfM-derived DoDs for subplots, whole survey area (All), and snow course. Differences between the snow depth median (cm) and the point measurement (Point) are presented in brackets.

Survey	Mire	Mixed	Forest	All	Snow course	Point
DEC-12	41 (6)	39 (4)	40 (5)	40 (5)	36 (1)	35
FEB-21	75 (−4)	75 (−4)	83 (4)	76 (−3)	75 (−4)	79
APR-03	77 (−11)	79 (−9)	84 (−4)	79 (−9)	85 (−3)	88
APR-24	36 (−28)	40 (−24)	56 (−8)	42 (−22)	43 (−21)	64

For APR-03, peat bog land cover shows no similarity with other land cover types, but other land cover types show similarities to each other. For APR-24 the differences between snow depth medians are highest, and similarity is indicated only for conifer forest and mixed forest with smaller sample sizes.

### 4.3 Vegetation interaction with snow depth

Figures 6 and 7 show the median snow depth as a function of distance from the canopy, zoomed in from 0 to 5 m for exploring canopy effects in detail, and zoomed out for the whole dataset up to approximately 50 m, respectively. Median snow depth was observed to generally increase with distance from the canopy at a proximity of 0.5 to 3 m (Fig. 6). This increase was moderate (3–5 cm) during the snow accumulation season (DEC-12 and FEB-21) and was reinforced

during the last two surveys at the beginning (APR-03) and in the middle (APR-24) of the melt period (up to +15 cm in forested areas). However, the increase remained moderate (2–8 cm) in peatland and transitional woodland/shrub covers for all survey times. After the peak, the snow depth started to decrease with distance from the canopy. The distance of the median snow depth maximum from the canopy (Fig. 6) was observed to increase in the snowmelt period (APR-03 and APR-24) to approximately 2.5 to 3 m, compared to 0.5 to 1 m in the snow accumulation period (DEC-12 and FEB-21), especially in mixed and coniferous forest areas.

After its maximum value, the median snow depth started to decrease at a rate somewhat depending on the land cover type and survey time (Figs. 6 and 7). This decrease was observed to be lowest in the snow accumulation period (DEC-12 and FEB-12) and reinforced in the snowmelt period (APR-03 and

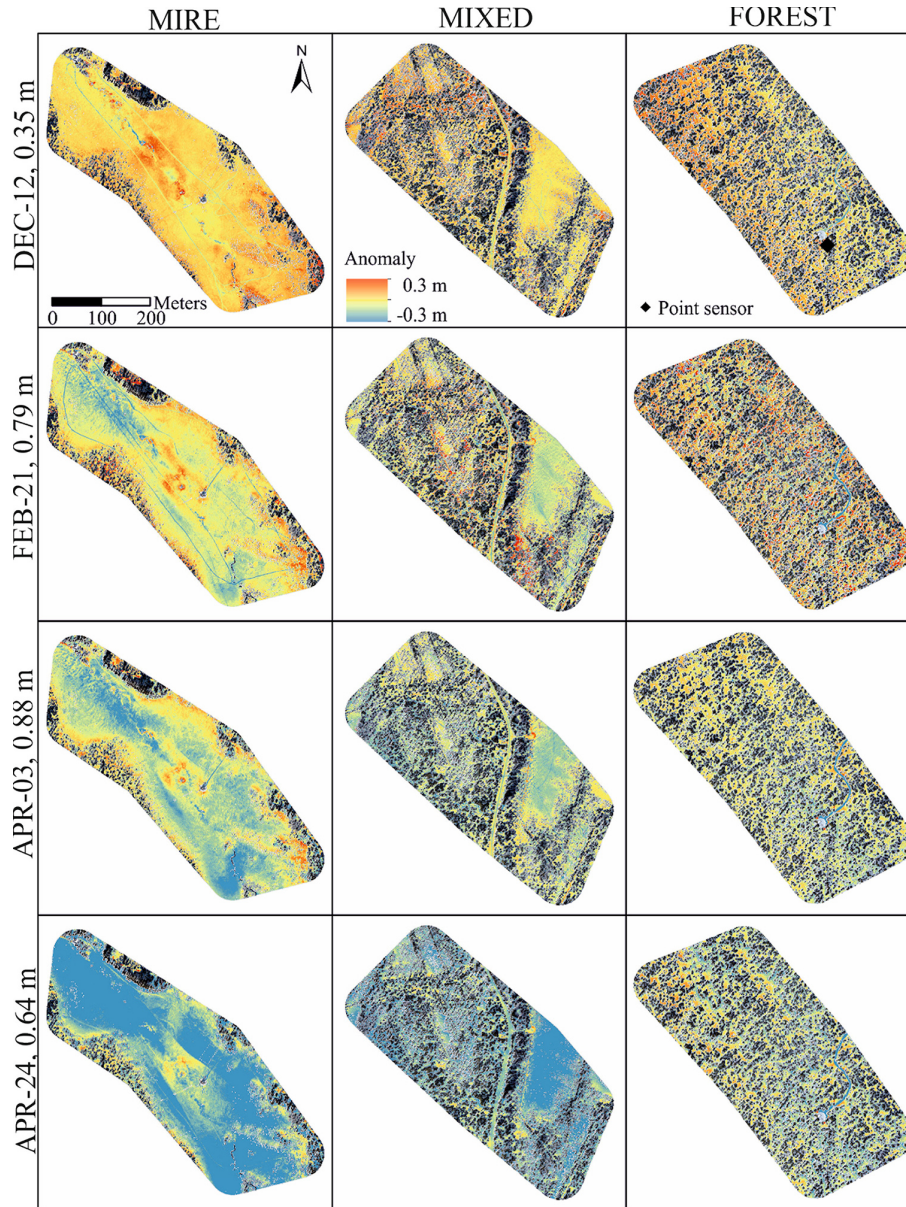


**Figure 4.** Snow depth (P4RTK snow – P4RTK ground) difference compared to point measurement at forest site. The point measurement is marked with a black dot in the forest site in the upper-right map. Snow depth from the point sensor is shown on the y axis after the survey date. Cold colors indicate areas where the snow depth is lower than the point measurement.

**Table 2.** Median snow depths and differences in snow depth (cm) between point measurement and UAS–SfM-derived DoDs for each land cover type and snow course measurements. Difference to point measurement (Point) is shown in brackets.

Survey	Peat bogs	Transitional wood/shrub	Mixed (and broad-leaved)	Coniferous	Snow course	Point
DEC-12	40 (5)	41 (6)	41 (6)	40 (5)	36 (1)	35
FEB-21	73 (–6)	78 (–1)	80 (1)	80 (1)	75 (–4)	79
APR-03	75 (–13)	83 (–5)	83 (–5)	82 (–6)	85 (–3)	88
APR-24	73 (–6)	42 (–22)	48 (–16)	51 (–13)	43 (–21)	64



**Table 3.** The 5th and 95th percentiles of snow depth (cm) and their range for UAS–SfM-derived DoDs and snow course measurements.

Survey	Peat bogs			Transitional wood/shrub			Mixed (and broad-leaved)			Coniferous			Snow course		
	5 %	95 %	Δ	5 %	95 %	Δ	5 %	95 %	Δ	5 %	95 %	Δ	5 %	95 %	Δ
DEC-12	31	48	17	32	51	19	27	62	35	24	57	33	31	46	15
FEB-21	58	87	29	63	95	32	59	125	66	54	116	62	70	86	16
APR-03	60	92	32	67	99	32	64	97	33	60	95	35	71	97	26
APR-24	12	54	42	21	63	42	23	69	46	20	69	49	0	59	59

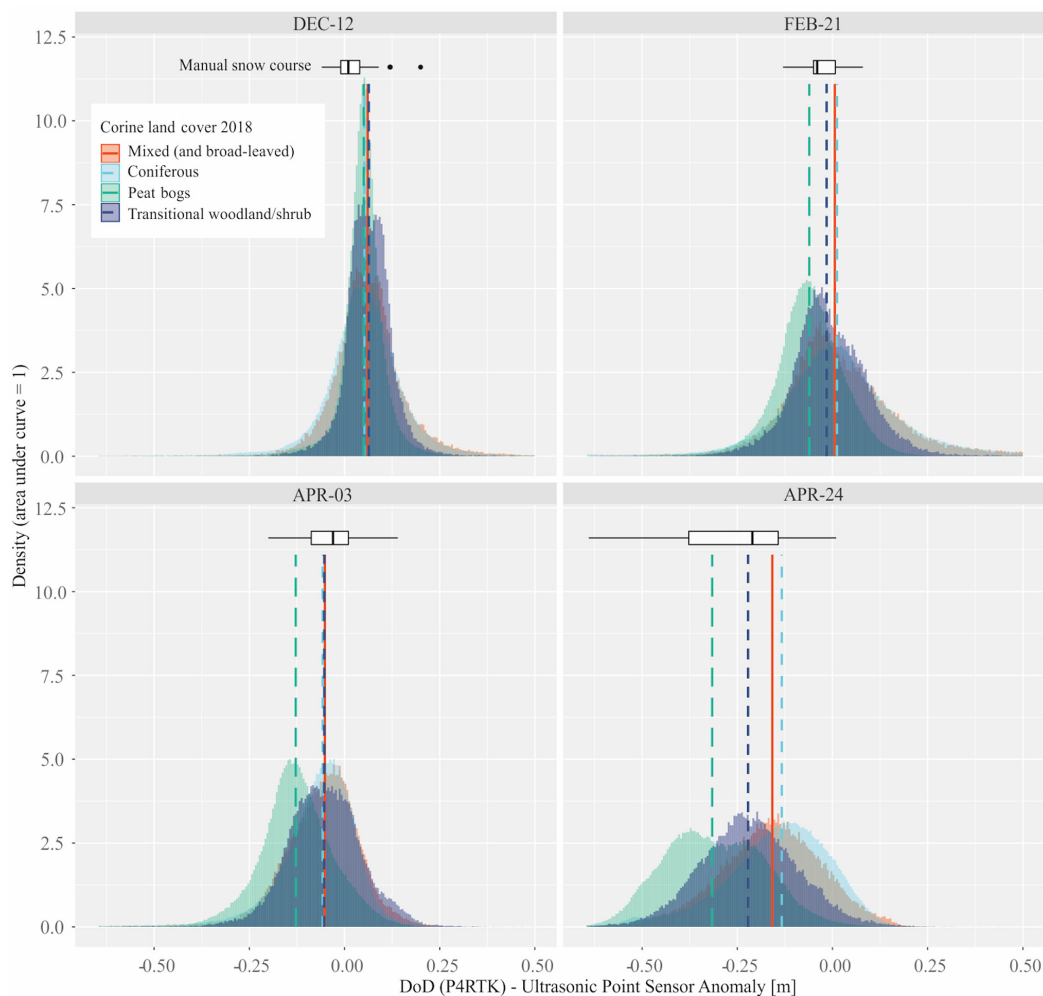


**Figure 5.** Snow depth difference (DoD P4RTK – ultrasonic point measurement) histograms for different Corine land cover types for all surveys. The boxplot shows difference data where Kenttäröva ultrasonic snow depth is subtracted from manual snow course measurement data in 46 locations. The dotted lines mark the median snow depths for each land cover type. Ultrasonic measurement is located at 0.0 on the x axis.

APR-24). The decrease continued generally to a 5–10 m distance from the canopy (Fig. 7). Subsequently, the variability in the snow depth was highest after 30 m from the canopy in peatland, where there could be bushes, and the number of pixels decreased. For the conifer forest, there is an anomalous and highly variable point cloud at 8–14 m from the canopy. In conifer, mixed forest, and transitional woodland/shrub the

snow depth had very low values between 5 and 10 m from the canopy.

Figure 8 shows the number of snow depth pixels, median snow depth, and the confidence interval (95 %) of the median snow depth as a function of distance from the canopy. The confidence interval and uncertainty of the median snow depth increases with the distance from the canopy as the number of

snow depth pixels decreases. For coniferous forest and mixed forest, the confidence interval widened substantially after 4–5 m; for transitional woodland/shrub this happened after 4 m and for peat bogs after 8 m distance from the canopy.

## 5 Discussion

### 5.1 Spatiotemporal variability in snow depth during accumulation and melt

In this study, we have successfully created high-resolution snow depth maps for the whole snowy season, covering snow accumulation and melt periods (from December to April) using the UAS–SfM method. As the generated snow depth maps compared favorably to conventional snow course surveys (difference in median snow depth between snow course and UAS–SfM-based data for the whole survey area being 4 cm in the early snow accumulation and 1 cm in the melt season period), the high-resolution method extends areal coverage, providing more detailed information of snow depth distribution and data for the snow process analysis. Moreover, the spatial variability shows the errors that may be associated with using point measurement as a regional reference for snow depth (Figs. 4 and 5). Regional snow depth/presence would be greatly overestimated (22 cm for whole survey area, varying from 28 cm in open peatland to 8 cm in forest) during the melt season if point measurement in the forest was used for regional reference. This could have major ramifications on operational flood estimates and simulations.

The UAS–SfM studies have so far mostly focused on the accuracy and precision analysis of the method, leaving spatial snow process considerations aside. This is especially true in boreal and subarctic landscapes, which are often comprised of a mosaic of forested, transitional, and peatland vegetated areas. However, attempts have been made to study the accuracy of the method in a defoliated spruce forest (Lendzioch et al., 2016), the accuracy of differential snow depth maps on ~ 50 m transects in sparse regenerating temperate broad-leaved and mixed forest (Fernandes et al., 2018), and the ability of UAS–SfM to observe subcanopy snow depth in temperate conifer forests (Harder et al., 2020). Instead of removing the forested areas or filtering the outliers from surface or snow depth maps, we used a tree mask to remove the noisy under- and near-canopy snow cover. These areas are problematic to UAS–SfM due to the mix of pixels on the snow surface and on the canopy, the difference in the canopy diameter with and without snow load, and broad-leaved trees that drop leaves in winter. Using the tree mask, we were successfully able to study snow depth dynamics in subarctic spruce forest areas. UAS–SfM techniques have typically been applied in single campaigns around the time of the deepest snow cover, or the focus has been on melt season. We, however, did measurements throughout the snow season, from early accumulation to melt season, allowing us to study

spatiotemporal variations in snow depth. This allowed us to quantify and compare differences in snow depth patterns and snow–canopy interaction in high resolution and under different snow conditions.

### 5.2 Snow depth variability for different land cover types

We observed differences in median snow depth (+5 to –32 cm compared to point measurement) and its range (from 17 to 49 cm) for different land cover types and found that it generally increased as the snow season progressed (Fig. 5, Tables 1 and 2). The range of snow depth was higher in forested areas compared to peatlands, matching the findings of Jost et al. (2007) for forests and clear-cuts. In the early phase of accumulation (DEC-12), the median snow depths were similar between land cover types, reflecting the similarity in surface texture and how the snow was trapped by the shrub on the peatlands. The low vegetation in open areas can hinder wind transport close to the ground (Liston et al., 2002), but its effect will diminish when the snow depth reaches its height. After that, the fallen snow is more subject to wind redistribution. However, compared to manual snow course and ultrasonic point reference measurements, the snow depth was overestimated by an average of +5 cm in the early phase of the snow accumulation (DEC-12). This is likely due to the snow-covered low vegetation being misclassified as snow surface (as observed in Fernandes et al., 2018), which was also visible in our orthophotos from the test sites (not shown).

In the middle (FEB-21) and the end (APR-03) of the snow accumulation season, the snow depth variability increased, and lower depths were observed, especially in peatlands (compared to other land cover types and ultrasonic point references). This can be explained by the wind-transport snow process both redepositing and sublimating snow (Pomeroy et al., 2002). Similar differences between open peatlands and forested areas were observed by Meriö et al. (2018). We observed increased snow depths at the edges of the peatlands (Fig. 4, see campaigns FEB-21 and APR-03 on mire), where forested areas slow the wind speeds, and the edges in proximity to the forest may act as a sink for the wind-transported snow (Hiemstra et al., 2002). These findings agreed with other studies (Hiemstra et al., 2002; Ketcheson et al., 2012).

The exceptionally high snow depth range in conifer (62 cm) and mixed (66 cm) forests for FEB-21 (Table 3, Fig. 5) was likely the result of snow on tree canopies causing anomalies in snow DEMs near the canopy. The SfM method faced challenges in these conditions, affecting snow depths beyond our tree masks, especially near broad-leaved trees where leafless branches could only partly be identified using supervised classification and thus not be removed completely by the tree mask (Fig. 4, more in Rauhala et al., 2023).

The variability in snow depth was highest in the middle of the melt period (APR-24) between and within the land

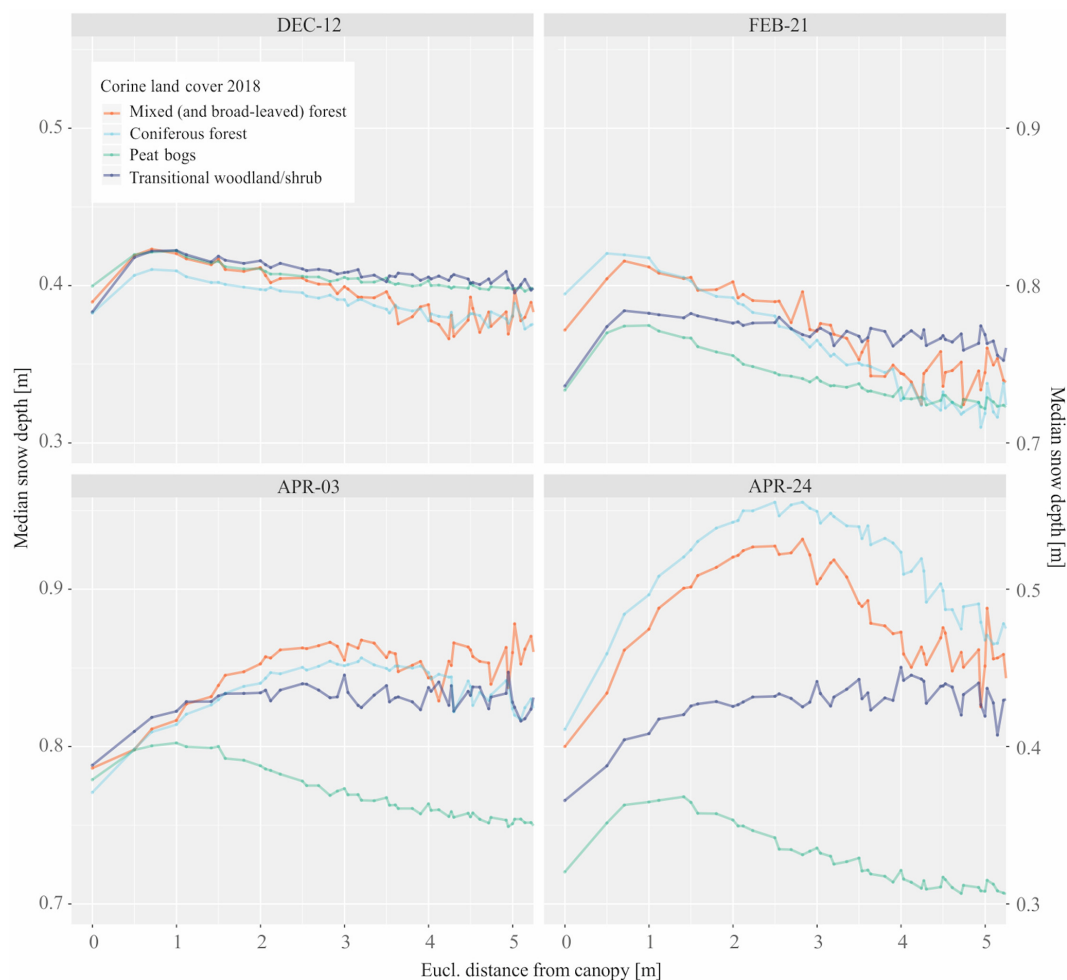


**Figure 6.** Zoomed euclidian distance from 0 to 5 m from the canopy (tree mask) for Corine land cover types in the test sites. The y-axis scale width is 0.26 m for all subfigures for comparable variability, but the min and max variation is similar for the pairs DEC-12 and APR-24 and FEB-21 and APR-03.

cover types, confirming earlier findings that spatial snow depth variability increases with time and scale (Neumann et al., 2006; Lopez-Moreno et al., 2015). In peatlands, the snow depth was lowest, explained by the lower initial snow depth at the beginning of the melt, likely caused by the wind drift, and the higher availability of energy for melt due to direct exposure to sunlight. The second lowest snow depth was found in transitional woodland/shrub, also hypothesized to be caused by melt due to high solar exposure (Hardy et al., 1997). The highest snow depths were found in conifer forests followed by mixed forests. This high depth was thought to be due to open areas, less direct shortwave radiation energy, and higher initial snow depth before melt (Lundquist and Lott, 2008). In the forested areas, the canopy cover was fairly low and interception was minor during the study winter, explaining the higher snow depths. Even though we do not have direct measurements of interception, our snow course survey

monitoring shows that the snow depths are typically higher in forested landscapes in different years.

At the end of the snow accumulation period and especially the middle of the melt period, the snow depths were substantially lower than the ultrasonic point measurement for forested and transitional land covers, highlighting the poor representativity of point measurements even for similar land cover types (Fig. 5). The representativeness of a point measurement location must be considered carefully, not only for a subcatchment scale but also for wider areas in operational or scientific use. The central value of and variability in the snow depth agreed generally well with manual snow course measurements, but the UAS-SfM snow depth maps expanded the spatial coverage substantially. Snow course measurements are limited in their ability to describe detailed canopy interactions with their low number of observations (tens to hundreds) compared to the UAS-SfM method (up to millions). Nonetheless, our analysis suggests that snow

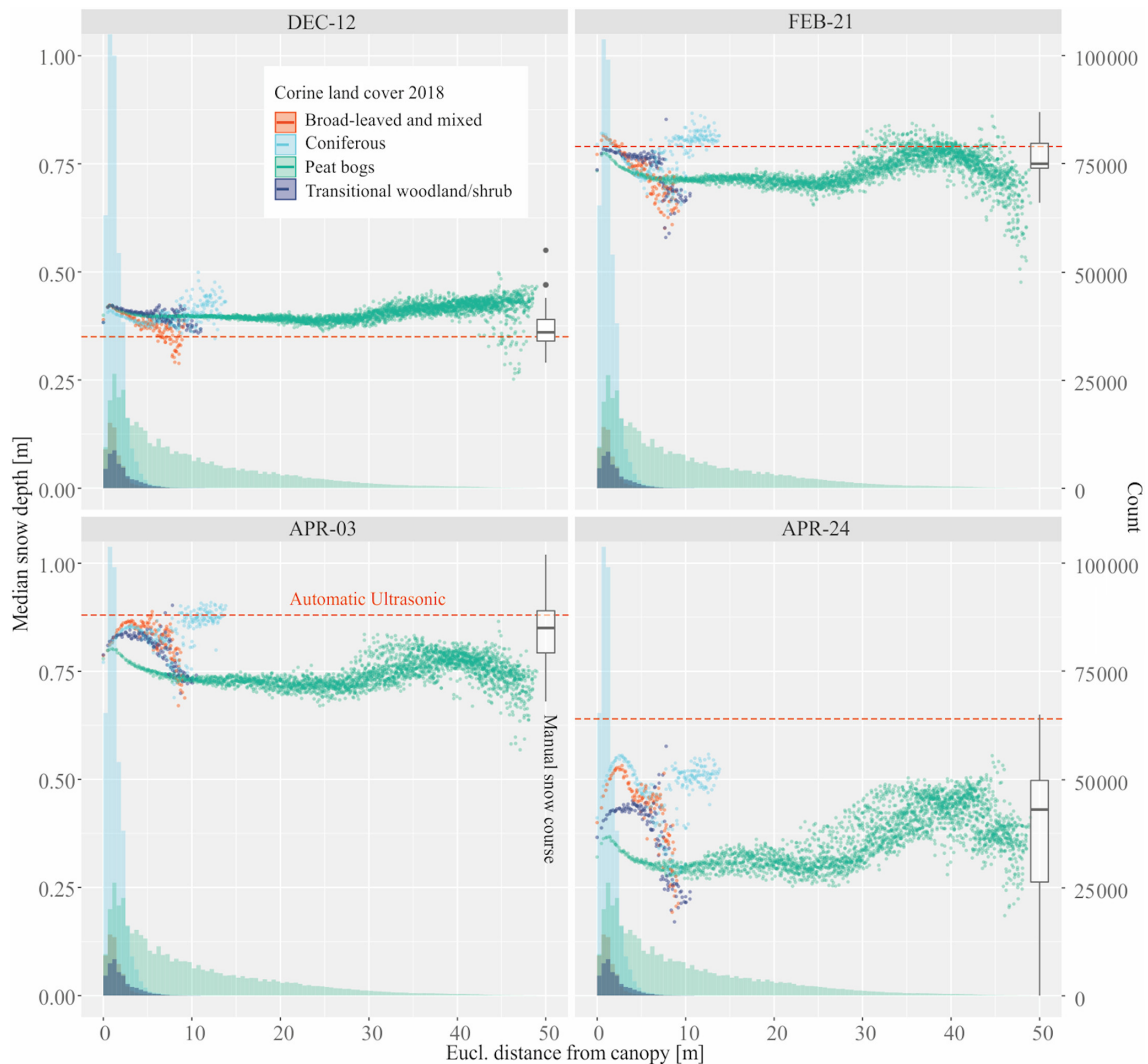


**Figure 7.** Median snow depth as a function of euclidian distance from the canopy (tree mask) for different Corine land cover types in the test sites. Boxplots show the manual snow course measurement data, and the dotted red line shows the measurement data from the ultrasonic sensor at Kenttäröva. Histograms show the count of snow depth pixels for each land cover type as a function of distance from the tree mask.

course, a widely used operational method for characterizing bulk snowpack (Pirazzini et al., 2018), produces a realistic picture of areal snow depth and its variability.

### 5.3 Vegetation interaction with snow depth

We found a systematic increase (from +2 to +15 cm) and then a decline in the median snow depth near the canopy (after the 0.36 m buffer from the canopy edge). Furthermore, we found an increasing distance of the peak value through the snow season (Fig. 6). This canopy interaction with snow cover is also documented by Pomeroy and Goodison (1997), who show how snow depth increases 10 cm from the edge of the branches to a 2 m distance for a white spruce, in a stand of trembling aspen. Similar findings were seen in sub-alpine forests by Musselman et al. (2008), who used normal-

ized snow depths around trees with a canopy radius of less than 2 and 4 m. A similar behavior is also indicated in the recent study near larch trees in Kananaskis, Alberta, Canada, by Harder et al. (2020). In forested areas, canopy interception and sublimation hinder the accumulation of snow under the canopy, which also affects the fringe area. Forest openings with dimensions from 2–5 times the height of the surrounding forest tend to collect the snow (Pomeroy et al., 2002). Tree trunks and canopies form shadowed areas but also absorb solar radiation and emit longwave radiation that can speed up the melt near trees (Faria et al., 2000; Lundquist et al., 2013).

Interestingly, with UAS-SfM-derived data we detected that the median snow depth had a peak value around 1 m from the tree mask during accumulation season, but this peak distance increased up to 2.5 m in the middle of the melt period.

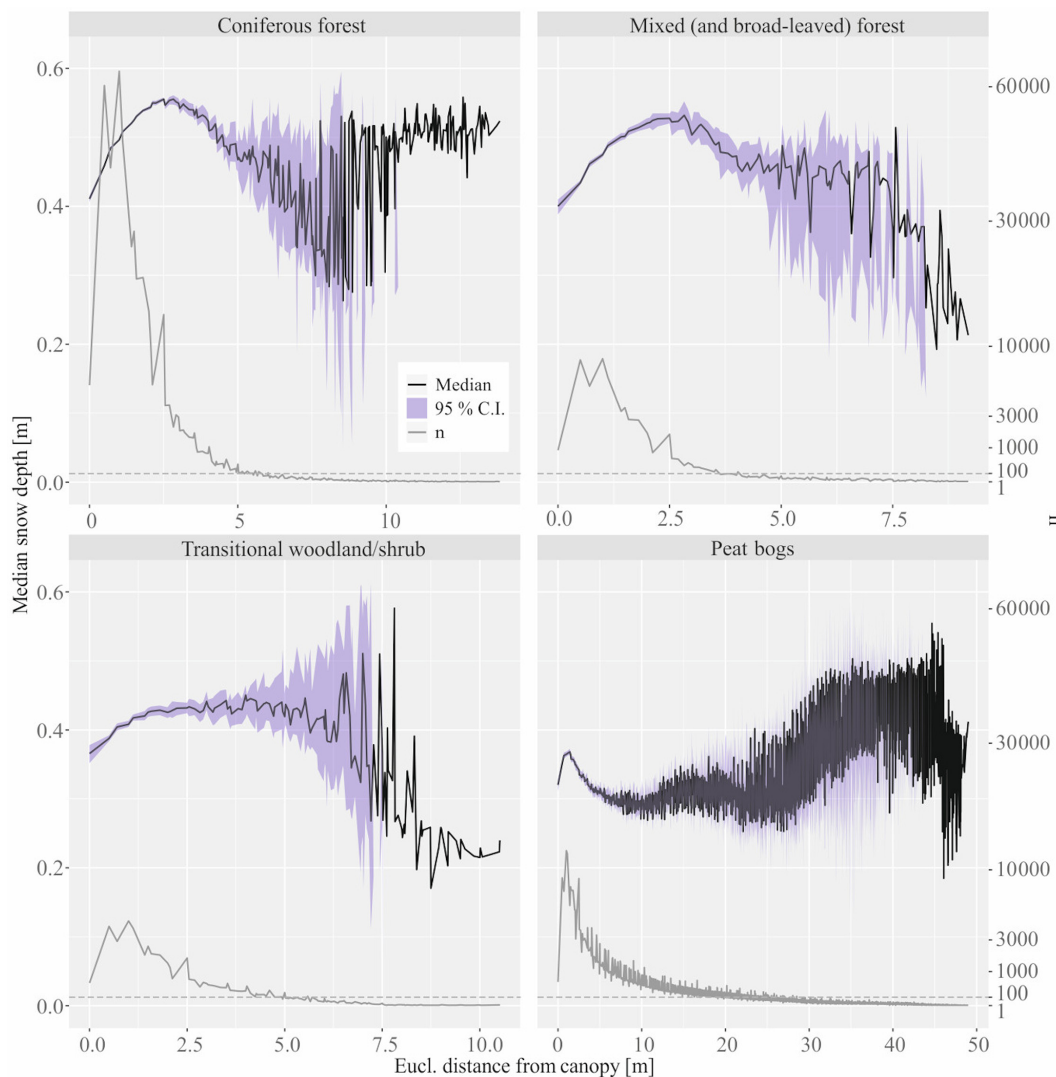


**Figure 8.** The confidence interval of median snow depth vs. distance from the canopy (tree mask) for different land cover types in survey APR-24. The 95 % confidence interval for the median is marked as a light violet band in the figure. The confidence band ends at the distance where the number of observations reduces to 1 or to a very small number of observations that are similar to each other. Dark gray shows the number ( $n$ ) of pixels for each distance. The dashed horizontal line marks 100 pixels.

After the peak, the snow depth decreased (Fig. 6). Moreover, the peak (from +2 cm for DEC-21 to +20 cm for APR-24) was intensified at the end of the melt period for conifer and mixed forests. This peak was less dramatic for mires and was not observed in transitional woodland/shrub. This variability could be explained by increased shortwave radiation towards spring being absorbed by the canopies, thus increasing the emitted longwave radiation that can increase the snowmelt rates near tree trunks. The longwave radiation is a function of tree temperature, which may be significantly different from air temperature and increase as spring progresses (Webster et al., 2016). Because the differences increase specifically during the melt period, we attribute the increase to the tree longwave radiation. During the snow accumulation period,

we propose the canopy interception to be the main driver in spatial snow depth variability. To our knowledge, this temporally changing snow–canopy interaction is not documented elsewhere.

For open peatland land cover, this snow depth peak near canopies may be explained by the wind distribution process that transports the snow to the edges of the open areas, where it is trapped by trees. A slight peak was observed for transitional woodland/shrub only after snowfall events for DEC-12 and FEB-21 but not for APR-03, when the compaction of snow after the last snowfall occurred on or before APR-24 when the snow was melting. This might be explained by the limited canopy effect compared with more densely forested conifer and mixed land cover, which may still hinder wind re-

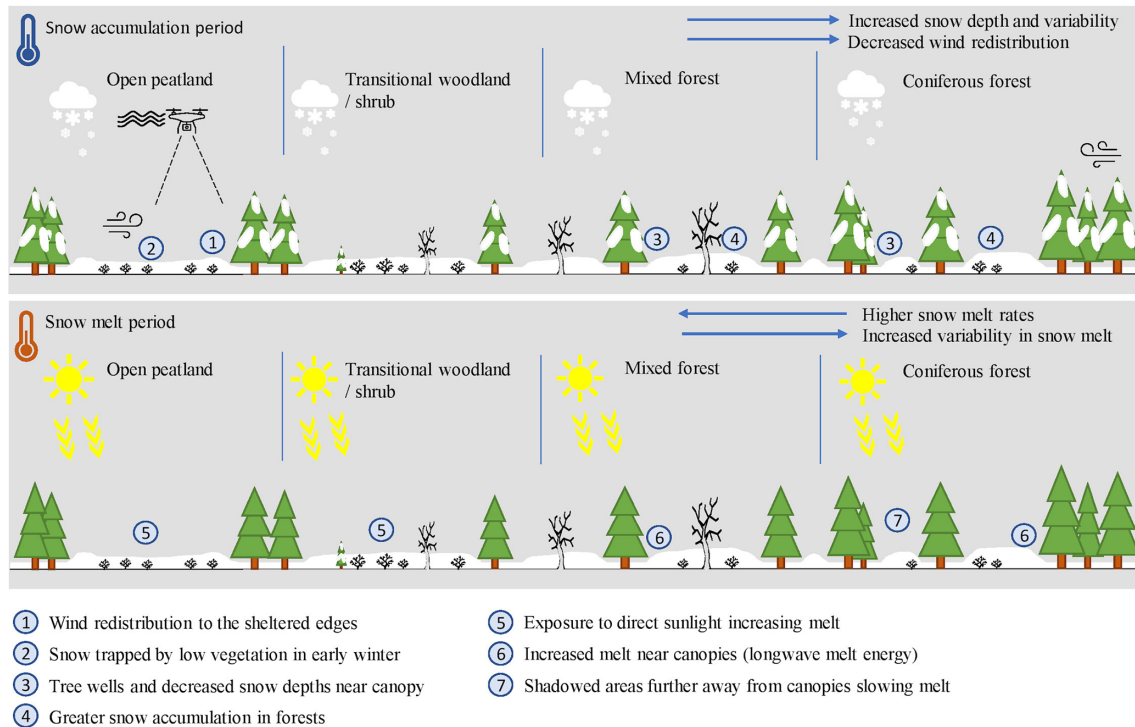


**Figure 9.** Observed snow accumulation and melt processes for different land cover types using the UAS–SfM method.

distribution compared to open areas. For conifer and mixed forest, the peak was clear during snow accumulation, especially for FEB-21, but decreased or was non-existent at the end of the accumulation season, APR-03 (Fig. 6). The effect was intensified in the middle of the melt period (APR-24), assumed to be caused by the combined impact of the trunk–canopy effect (longwave melt energy) extending further from the canopy and direct solar radiation affecting the northern side of the forest openings, while the southern sides were protected by shadows (Faria et al., 2000; Essery et al., 2008). This may create asymmetric snow depth patterns (Fig. 4, APR-24) that are shown as decreased snow depths after 3 m from the tree mask. Moreover, the uncertainty is increased after a 2.5–3 m distance from the tree mask, especially for forested and transitional woodland areas because the number of pixels for those distances decreased substantially (Fig. 8). Thus, the snow depth decrease for APR-24 after 3 m from the tree mask in forested areas remains unexplained. The observed snow processes for different land cover types and snow–canopy interactions for the snow accumulation and melt periods are summarized in Fig. 9.

The anomalies between 5 and 14 m from the canopy (Fig. 7) were thought to be partly misclassified Corine land cover pixels: conifer forest pixels at the edge of the peatland (mire site), conifer forest pixels at the edge of the peatland (mixed site) and the road to the FMI Kenttäröva measurement station (forest site), mixed forest pixels at the edge of

the peatland (mire site), and transitional woodland/shrub pixels at the edge of the peatland (mixed site).

#### 5.4 Opportunities and challenges in determining snow processes using UAS–SfM

Our results highlight how the UAS–SfM method can be used for frequent, high-spatial-resolution snow depth coverage in a cost-efficient manner. The key advantage is that the method allows for the measurement of snow depth with high position accuracy (at a centimeter scale) throughout the landscape, which in our 0.5 m resolution maps resulted in 917 045 approximations of snow depth for a 23 ha area. This is at least an order of magnitude higher than other established methods, such as snow surveys with automated magnaprobe (1000–10 000 measurement points; Sturm and Holmgren, 2018), snow surveys with manual probes (10–100 measurements; Lundberg and Koivusalo 2003; Pirazzini et al., 2018), or continuous point measurements (1–10 measurement points; Zhang et al., 2017). The position accuracy of these other established methods is typical  $\pm 3$  m, which is done using standard GNSS.

A large number of points with high position accuracy allows for the detailed snow process analysis in relatively large areas or even up to small catchments using fixed-wing UASs, as well as within and between different land cover types that are not easily possible with other methods, such as manual snow course measurements. Airborne lidar has been used for

similar analysis with the advantage of canopy penetration but with a cost which is an order of magnitude higher (Harder et al., 2020). By removing the parts containing forest canopies with a small buffer, the UAS–SfM method allows for the analysis of snow–vegetation interactions for forested areas and larger trees. The observed snow depth peak, especially in forested areas during melt, requires more study and observation.

The greatest challenges in using the UAS–SfM method are related to vegetation, weather, and the reflectance properties of fresh snow. To minimize the vegetation effect, it is recommended to do a bare-ground survey soon after snowmelt, when the vegetation is still compact and the growing season has not started. An airborne lidar survey of the ground would again allow penetration of the vegetation at a high cost, but we found (Rauhala et al., 2023) that the difference was minor when tree masks were used to remove larger vegetation. For forested areas, cameras with near-infrared (NIR) frequency bands could help in tree mask creation, using supervised classification, especially for broad-leaved trees whose branches are sometimes mixed with shadows and debris on snow cover. During the midwinter, the limited daylight hours in high latitudes must also be considered, as they limit good windows for measurements. The NIR band could further improve snow pixel identification under challenging illumination conditions by avoiding holes in the point cloud caused by missing key points (Adams et al., 2018). The light conditions and extreme cold weather pose a particular challenge in the northern boreal zone. The issues related to this dataset are addressed in detail by Rauhala et al. (2023).

The high-resolution snow depth maps generated using the UAS–SfM method could further be used in small-scale (below 1 to 100 m) studies of snow accumulation and melt processes, including enhanced observation of interactions between snow, vegetation, and topography. On a local or medium scale (100–4000 m), the method could be used to improve landscape-specific information for snow depth for recreational use and tourism, as well as in calibrating and/or validating catchment-scale hydrological models used in research, environmental planning, hydropower, or flood prediction (Kinar and Pomeroy 2015; Sturm, 2015; Ala-aho et al., 2017; Hewer and Gough, 2018).

## 6 Conclusions

This study extends the coverage of UAS–SfM studies to the subarctic region with multiple surveys through the snow accumulation and melt season under different weather conditions. Our high-resolution data underline the potential biases in point-scale snow monitoring. The observations show increasing differences from early snow accumulation to the middle of the melt season. For all land cover types, the bias changed in time, from +5 cm in the early snow accumulation period to –16 cm in forests and –32 cm in peatland in

the middle of the melt period. This highlights the poor representation of single-point measurements even on the sub-catchment level or a poorly selected measurement location.

The multiple-campaign approach allowed us to show how the spatial variability in snow depth increases as the snow season progresses. The land-cover-specific snow depth range (5th–95th percentiles) increased from 33 to 49 cm in forests and from 17 to 42 cm in peatlands from early winter to the melt season. The high-spatial-resolution data offered new insights into theoretically known snow processes and interactions between snow and vegetation at the landscape scale. Canopy interception, long-wave radiation emitted by the trees, and wind transport with deposition of snow at forest edges, for both forested and peatland areas, contributed to the snow depth variability. The effect of decreased snow accumulation, which was reinforced from early accumulation to the middle of the melt season from 2 to 20 cm and below canopies extending outside the immediate canopy from 1 to 2.5 m, respectively, was also shown in a high-resolution, spatially extensive analysis.

Our study highlights the applicability of the UAS–SfM method to be used for a detailed study of snow depth in multiple land cover types, including sparse subarctic forest and vegetation boundaries. The generated tree masks to remove trees and the areas immediately next to trees, which is challenging for snow remote sensing, allowed the usage of the UAS–SfM methodology in tree-covered areas and can be recommended for future use. While we found that the widely used snow course data produced a realistic picture of areal snow depth conditions that can be used in operational services, the UAS–SfM-derived data can be used to extend the spatial scale of snow course measurements, in snow model calibration and validation on a catchment scale, and to improve forecasts for operational and decision-making purposes.

*Data availability.* The data underlying this analysis and its documentation are available at <https://doi.org/10.23729/43d37797-e8cf-4190-80f1-ff567ec62836> (Rauhala et al., 2022) under a Creative Commons CC-BY-4.0 license.

*Supplement.* The supplement related to this article is available online at: <https://doi.org/10.5194/tc-17-4363-2023-supplement>.

*Author contributions.* LJM, HM, PA, and AR designed the field studies, while LJM, AR, AK, and PK carried them out and processed the data. LJM analyzed the data and prepared the manuscript with contributions from all co-authors. HM, TK, and PA supervised the research.

*Competing interests.* The contact author has declared that none of the authors has any competing interests.

*Disclaimer.* Publisher's note: Copernicus Publications remains neutral with regard to jurisdictional claims in published maps and institutional affiliations.

*Acknowledgements.* We thank Valtteri Höyky and Metsähallitus for assisting with field sampling campaigns. We gratefully acknowledge the field work assistance of Filip Muhic, Kashif Noor, Aleksi Ritakallio, Alexandre Pepy, Jari-Pekka Nousu, and Valtteri Hyöky.

*Financial support.* This study was supported by the Maa-ja vesitekniiikan tuki ry, K. H. Renlund Foundation, Academy of Finland (projects 316349, 330319, and ArcI Profi 4); the Strategic Research Council (SRC) decision no. 312636 (IBC-Carbon); EU Horizon 2020 Research and Innovation Programme grant agreement no. 869471; and the Kvantum Institute at the University of Oulu.

*Review statement.* This paper was edited by Carrie Vuyovich and reviewed by two anonymous referees.

## References

- Adams, M. S., Bühler, Y., and Fromm, R.: Multitemporal accuracy and precision assessment of unmanned aerial system photogrammetry for slope-scale snow depth maps in Alpine terrain, *Pure Appl. Geophys.*, 175, 3303–3324, <https://doi.org/10.1007/s00024-017-1748-y>, 2018.
- Agisoft: AgiSoft Metashape Professional (Version 1.6.0), Agisoft [software], <https://www.agisoft.com/downloads/installer/> (last access: 8 September 2019), 2019.
- Agisoft: Agisoft Metashape User Manual: Professional Edition, Version 2.0. Agisoft LLC, [https://www.agisoft.com/pdf/metashape-pro\\_2\\_0\\_en.pdf](https://www.agisoft.com/pdf/metashape-pro_2_0_en.pdf) (last access: 25 May 2023), 2023.
- Ala-aho, P., Tetzlaff, D., McNamara, J. P., Laudon, H., Kormos, P., and Soulsby, C.: Modeling the isotopic evolution of snowpack and snowmelt: Testing a spatially distributed parsimonious approach, *Water Resour. Res.*, 53, 5813–5830, <https://doi.org/10.1002/2017WR020650>, 2017.
- Blume-Werry, G., Kreyling, J., Laudon, H., and Milbau, A.: Short-term climate change manipulation effects do not scale up to long-term legacies: Effects of an absent snow cover on boreal forest plants, *J. Ecol.*, 104, 1638–1648, <https://doi.org/10.1111/1365-2745.12636>, 2016.
- Brown, R. D. and Robinson, D. A.: Northern Hemisphere spring snow cover variability and change over 1922–2010 including an assessment of uncertainty, *The Cryosphere*, 5, 219–229, <https://doi.org/10.5194/tc-5-219-2011>, 2011.
- Bühler, Y., Adams, M. S., Bösch, R., and Stoffel, A.: Mapping snow depth in alpine terrain with unmanned aerial systems (UASs): potential and limitations, *The Cryosphere*, 10, 1075–1088, <https://doi.org/10.5194/tc-10-1075-2016>, 2016.
- Clark, M. P., Hendriks, J., Slater, A. G., Kavetski, D., Anderson, B., Cullen, N. J., Kerr, T., Örn Hreinsson, E., and Woods, R. A.: Representing spatial variability of snow water equivalent in hydrologic and land-surface models: A review, *Water Resour. Res.*, 47, W07539, <https://doi.org/10.1029/2011WR010745>, 2011.
- Deems, J. S. and Painter, T. H.: Lidar measurement of snow depth: accuracy and error sources, *Proceedings of the 2006 International Snow Science Workshop*, Telluride, Colorado, USA, International Snow Science Workshop, 330–338, 1–6 October 2006.
- Deems, J. S., Painter, T. H., and Finnegan, D. C.: Lidar measurement of snow depth: a review, *J. Glaciol.*, 59, 467–479, <https://doi.org/10.3189/2013JoG12J154>, 2013.
- De Michele, C., Avanzi, F., Passoni, D., Barzaghi, R., Pinto, L., Dosso, P., Ghezzi, A., Gianatti, R., and Della Vedova, G.: Using a fixed-wing UAS to map snow depth distribution: an evaluation at peak accumulation, *The Cryosphere*, 10, 511–522, <https://doi.org/10.5194/tc-10-511-2016>, 2016.
- Dietz, A. J., Kuenzer, C., Gessner, U., and Dech, S.: Remote sensing of snow – a review of available methods, *Int. J. Remote Sens.*, 33, 4094–4134, <https://doi.org/10.1080/01431161.2011.640964>, 2012.
- Dunn, O. J.: Multiple comparisons among means, *J. Am. Stat. Assoc.*, 56, 52–64, 1961.
- Dunn, O. J.: Multiple comparisons using rank sums, *Technometrics*, 6, 241–252, <https://doi.org/10.2307/1266041>, 1964.
- Earman, S., Campbell, A. R., Phillips, F. M., and Newman, B. D.: Isotopic exchange between snow and atmospheric water vapor: Estimation of the snowmelt component of groundwater recharge in the southwestern United States, *J. Geophys. Res.-Atmos.*, 111, D09302, <https://doi.org/10.1029/2005JD006470>, 2006.
- EEA: European Union, Copernicus land monitoring service 2018, European environment agency, 2018.
- Esri: ArcGIS Desktop (Version 10.6) (Software), <https://www.esri.com/en-us/arcgis/products/arcgis-desktop/overview> (last access: 6 August 2019), 2019.
- Essery, R., Bunting, P., Rowlands, A., Rutter, N., Hardy, J., Melloh, R., Link, T., Marks, D., and Pomeroy, J.: Radiative transfer modeling of a coniferous canopy characterized by airborne remote sensing, *J. Hydrometeorol.*, 9, 228–241, <https://doi.org/10.1175/2007JHM870.1>, 2008.
- Faria, D. A., Pomeroy, J. W., and Essery, R. L. H.: Effect of covariance between ablation and snow water equivalent on depletion of snow-covered area in a forest, *Hydrol. Process.*, 14, 2683–2695, [https://doi.org/10.1002/1099-1085\(20001030\)14:15<2683::AID-HYP86>3.0.CO;2-N](https://doi.org/10.1002/1099-1085(20001030)14:15<2683::AID-HYP86>3.0.CO;2-N), 2000.
- Feiccabrino, J. and Lundberg, A.: Precipitation phase discrimination in Sweden, 65th Eastern Snow Conference, Fairlee (Lake Morey), Vermont, USA, Abstract No. 18, 28–30 May 2008, 2008.
- Fernandes, R., Prevost, C., Canisius, F., Leblanc, S. G., Maloley, M., Oakes, S., Holman, K., and Knudby, A.: Monitoring snow depth change across a range of landscapes with ephemeral snowpacks using structure from motion applied to lightweight unmanned aerial vehicle videos, *The Cryosphere*, 12, 3535–3550, <https://doi.org/10.5194/tc-12-3535-2018>, 2018.
- Gary, H. L.: Snow accumulation and snowmelt as influenced by a small clearing in a lodgepole pine forest, *Water Resour. Res.*, 10, 348–353, <https://doi.org/10.1029/WR010i002p00348>, 1974.
- Gelfan, A. N., Pomeroy, J. W., and Kuchment, L. S.: Modeling forest cover influences on snow accumulation, sublimation, and melt, *J. Hydrometeorol.*



- teorol., 5, 785–803, [https://doi.org/10.1175/1525-7541\(2004\)005<0785:MFCIOS>2.0.CO;2](https://doi.org/10.1175/1525-7541(2004)005<0785:MFCIOS>2.0.CO;2), 2004.
- Godsey, S. E., Kirchner, J. W., and Tague, C. L.: Effects of changes in winter snowpacks on summer low flows: case studies in the Sierra Nevada, California, USA, *Hydrol. Process.*, 28, 5048–5064, <https://doi.org/10.1002/hyp.9943>, 2014.
- Golding, D. L. and Swanson, R. H.: Snow accumulation and melt in small forest openings in Alberta, *Can. J. Forest Res.*, 8, 380–388, <https://doi.org/10.1139/x78-057>, 1978.
- Harder, P., Pomeroy, J. W., and Helgason, W. D.: Improving sub-canopy snow depth mapping with unmanned aerial vehicles: lidar versus structure-from-motion techniques, *The Cryosphere*, 14, 1919–1935, <https://doi.org/10.5194/tc-14-1919-2020>, 2020.
- Hardy, J. P., Davis, R. E., Jordan, R., Li, X., Woodcock, C., Ni, W., and McKenzie, J. C.: Snow ablation modeling at the stand scale in a boreal jack pine forest, *J. Geophys. Res.-Atmos.*, 102, 29397–29405, <https://doi.org/10.1029/96JD03096>, 1997.
- Hewer, M. J. and Gough, W. A.: Thirty years of assessing the impacts of climate change on outdoor recreation and tourism in Canada, *Tourism Management Perspectives*, 26, 179–192, <https://doi.org/10.1016/j.tmp.2017.07.003>, 2018.
- Hiemstra, C. A., Liston, G. E., and Reiners, W. A.: Snow redistribution by wind and interactions with vegetation at upper treeline in the Medicine Bow Mountains, Wyoming, USA, *Arct. Antarct. Alp. Res.*, 34, 262–273, <https://doi.org/10.1080/15230430.2002.12003493>, 2002.
- Jenicek, M., Seibert, J., Zappa, M., Staudinger, M., and Jonas, T.: Importance of maximum snow accumulation for summer low flows in humid catchments, *Hydrol. Earth Syst. Sci.*, 20, 859–874, <https://doi.org/10.5194/hess-20-859-2016>, 2016.
- Jost, G., Weiler, M., Gluns, D. R., and Alila, Y.: The influence of forest and topography on snow accumulation and melt at the watershed-scale, *J. Hydrol.*, 347, 101–115, <https://doi.org/10.1016/j.jhydrol.2007.09.006>, 2007.
- Ketcheson, S. J., Whittington, P. N., and Price, J. S.: The effect of peatland harvesting on snow accumulation, ablation and snow surface energy balance, *Hydrol. Process.*, 26, 2592–2600, <https://doi.org/10.1002/hyp.9325>, 2012.
- Kinar, N. J. and Pomeroy, J. W.: Measurement of the physical properties of the snowpack, *Rev. Geophys.*, 53, 481–544, <https://doi.org/10.1002/2015RG000481>, 2015.
- Lendziach, T., Langhammer, J., and Jenicek, M.: Tracking forest and open area effects on snow accumulation by unmanned aerial vehicle photogrammetry, *Int. Arch. Photogramm. Remote Sens. Spatial Inf. Sci.*, XLI-B1, 917–923, <https://doi.org/10.5194/isprsarchives-XLI-B1-917-2016>, 2016.
- Lievens, H., Demuzere, M., Marshall, H. P., Reichle, R. H., Brucker, L., Brangers, I., de Rosnay, P., Dumont, M., Giroto, M., Immerzeel, W. W., Jonas, T., Kim, E. J., Koch, I., Marty, C., Saloranta, T., Schöber, J. and De Lannoy, G. J. M.: Snow depth variability in the Northern Hemisphere mountains observed from space, *Nat. Commun.*, 10, 1–12, <https://doi.org/10.1038/s41467-019-12566-y>, 2019.
- Lin, M., Lucas Jr, H. C., and Shmueli, G.: Research commentary – too big to fail: large samples and the p-value problem, *Inf. Syst. Res.*, 24, 906–917, <https://doi.org/10.1287/isre.2013.0480>, 2013.
- Liston, G. E.: Interrelationships among snow distribution, snowmelt, and snow cover depletion: Implications for atmospheric, hydrologic, and ecologic modelling, *J. Appl. Meteorol.*, 38, 1474–1487, [https://doi.org/10.1175/1520-0450\(1999\)038<1474:IASDSA>2.0.CO;2](https://doi.org/10.1175/1520-0450(1999)038<1474:IASDSA>2.0.CO;2), 1999.
- Liston, G. E., Mcfadden, J. P., Sturm, M., and Pielke, R. A.: Modelled changes in arctic tundra snow, energy and moisture fluxes due to increased shrubs, *Glob. Change Biol.*, 8, 17–32, <https://doi.org/10.1046/j.1354-1013.2001.00416.x>, 2002.
- López-Moreno, J. I., Revuelto, J., Fassnacht, S. R., Azorín-Molina, C., Vicente-Serrano, S. M., Morán-Tejeda, E., and Sextstone, G. A.: Snowpack variability across various spatio-temporal resolutions, *Hydrol. Process.*, 29, 1213–1224, <https://doi.org/10.1002/hyp.10245>, 2015.
- Lundberg, A. and Koivusalo, H.: Estimating winter evaporation in boreal forests with operational snow course data, *Hydrol. Process.*, 17, 1479–1493, <https://doi.org/10.1002/hyp.1179>, 2003.
- Lundquist, J. D. and Lott, F.: Using inexpensive temperature sensors to monitor the duration and heterogeneity of snow-covered areas, *Water Resour. Res.*, 44, W00D16, <https://doi.org/10.1029/2008WR007035>, 2008.
- Lundquist, J. D., Dickerson-Lange, S. E., Lutz, J. A., and Cristea, N. C.: Lower forest density enhances snow retention in regions with warmer winters: A global framework developed from plot-scale observations and modelling, *Water Resour. Res.*, 49, 6356–6370, <https://doi.org/10.1002/wrcr.20504>, 2013.
- Luomaranta, A., Aalto, J., and Jylhä, K.: Snow cover trends in Finland over 1961–2014 based on gridded snow depth observations, *Int. J. Climatol.*, 39, 3147–3159, <https://doi.org/10.1002/joc.6007>, 2019.
- Mankin, J. S., Viviroli, D., Singh, D., Hoekstra, A. Y., and Diffenbaugh, N. S.: The potential for snow to supply human water demand in the present and future, *Environ. Res. Lett.*, 10, 114016, <https://doi.org/10.1088/1748-9326/10/11/114016>, 2015.
- Marttila, H., Lohila, A., Ala-aho, P., Noor, K., Welker, J.M., Croghan, D., Mustonen, K., Meriö, L.J., Autio, A., Muhic, F., Bailey, H., Aurela, M., Vuorenmaa, J., Penttilä, T., Hyöky, V., Klein, E., Kuzmin, A., Korpelainen, P., Kumpula, T., Rauhala, A., and Kløve, B.: Subarctic catchment water storage and carbon cycling – Leading the way for future studies using integrated datasets at Pallas, Finland, *Hydrol. Process.*, 35, e14350, <https://doi.org/10.1002/hyp.14350>, 2021.
- McKay, G. A. and Gray, D. M.: The distribution of snow cover, in: *Handbook of Snow: Principles, Process, Management and Use*, Illustrated edition, edited by: Gray, D. M. and Male, D. H., Blackburn Press, 153–190, ISBN 9781932846065, 2004.
- Meriö, L. J., Marttila, H., Ala-aho, P., Hänninen, P., Okkonen, J., Sutinen, R., and Kløve, B.: Snow profile temperature measurements in spatiotemporal analysis of snowmelt in a subarctic forest-mire hillslope, *Cold Reg. Sci. Technol.*, 151, 119–132, <https://doi.org/10.1016/j.coldregions.2018.03.013>, 2018.
- Mudryk, L., Santolaria-Otín, M., Krinner, G., Ménégos, M., Derksen, C., Brutel-Vuilmet, C., Brady, M., and Essery, R.: Historical Northern Hemisphere snow cover trends and projected changes in the CMIP6 multi-model ensemble, *The Cryosphere*, 14, 2495–2514, <https://doi.org/10.5194/tc-14-2495-2020>, 2020.
- Musselman, K. N., Molotch, N. P., and Brooks, P. D.: Effects of vegetation on snow accumulation and ablation in a mid-latitude sub-alpine forest, *Hydrol. Process.*, 22, 2767–2776, <https://doi.org/10.1002/hyp.7050>, 2008.

- Musselman, K. N., Clark, M. P., Liu, C., Ikeda, K., and Rasmussen, R.: Slower snowmelt in a warmer world, *Nat. Clim. Change*, 7, 214–219, <https://doi.org/10.1038/nclimate3225>, 2017.
- Neumann, N.N., Derksen, C., Smith, C., and Goodison, B.: Characterizing local scale snow cover using point measurements during the winter season, *Atmos. Ocean*, 44, 257–269, <https://doi.org/10.3137/ao.440304>, 2006.
- Neuvonen, M., Sievänen, T., Fronzek, S., Lahtinen, I., Veijalainen, N., and Carter, T. R.: Vulnerability of cross-country skiing to climate change in Finland—An interactive mapping tool, *J. Outdoor Recreat. Tour.*, 11, 64–79, <https://doi.org/10.1016/j.jort.2015.06.010>, 2015.
- Niedzielski, T., Szymanowski, M., Miziński, B., Spallek, W., Witek-Kasprzak, M., Ślopek, J., Kasprzak, M., Błaś, M., Sobik, M., Jancewicz, K., and Borowicz, D.: Estimating snow water equivalent using unmanned aerial vehicles for determining snow-melt runoff, *J. Hydrol.*, 578, 124046, <https://doi.org/10.1016/j.jhydrol.2019.124046>, 2019.
- Pirazzini, R., Leppänen, L., Picard, G., Lopez-Moreno, J. I., Marty, C., Macelloni, G., Kontu, A., Von Lerber, A., Tanis, C. M., Schneebeli, M., and De Rosnay, P.: European in-situ snow measurements: Practices and purposes, *Sensors*, 18, 2016, <https://doi.org/10.3390/s18072016>, 2018.
- Pomeroy, J. W. and Brun, E.: Physical properties of snow, in: *Snow ecology: An interdisciplinary examination of snow-covered ecosystems*, edited by: Jones, H. G., Pomeroy, J. W., Walker, D. A., and Homan, R. W., Cambridge University Press, Cambridge, 45–126, ISBN 9780521584838, 2001.
- Pomeroy, J. W. and Goodison, B. E.: Winter and snow, in: *The Surface Climates of Canada*, edited by: Bailey, W. G., Oke, T. R., and Rouse, W. R., McGill-Queen's Press, 68–100, ISBN 9780773516724, 1997.
- Pomeroy, J. W., Gray, D. M., Hedstrom, N. R., and Janowicz, J. R.: Prediction of seasonal snow accumulation in cold climate forests, *Hydrol. Process.*, 16, 3543–3558, <https://doi.org/10.1002/hyp.1228>, 2002.
- Pulliaainen, J., Luojus, K., Derksen, C., Mudryk, L., Lemmetyinen, J., Salminen, M., Ikonen, J., Takala, M., Cohen, J., Smolander, T., and Norberg, J.: Patterns and trends of northern hemisphere snow mass from 1980 to 2018, *Nature*, 581, 294–298, <https://doi.org/10.1038/s41586-020-2258-0>, 2020.
- Rauhala, A., Meriö, L. J., Korpelainen, P., and Kuzmin, A.: Unmanned aircraft system (UAS) snow depth mapping at the Pallas Atmosphere-Ecosystem Supersite, Fairdata [data set], <https://doi.org/10.23729/43d37797-e8cf-4190-80f1-ff567ec62836>, 2022.
- Rauhala, A., Meriö, L.-J., Kuzmin, A., Korpelainen, P., Alahö, P., Kumpula, T., Kløve, B., and Marttila, H.: Measuring the spatiotemporal variability in snow depth in subarctic environments using UASs – Part 1: Measurements, processing, and accuracy assessment, *The Cryosphere*, 17, 4343–4362, <https://doi.org/10.5194/tc-17-4343-2023>, 2023.
- Redpath, T. A. N., Sirguey, P., and Cullen, N. J.: Repeat mapping of snow depth across an alpine catchment with RPAS photogrammetry, *The Cryosphere*, 12, 3477–3497, <https://doi.org/10.5194/tc-12-3477-2018>, 2018.
- Schirmer, M. and Pomeroy, J. W.: Processes governing snow ablation in alpine terrain – detailed measurements from the Canadian Rockies, *Hydrol. Earth Syst. Sci.*, 24, 143–157, <https://doi.org/10.5194/hess-24-143-2020>, 2020.
- Scott, D., Dawson, J., and Jones, B.: Climate change vulnerability of the US Northeast winter recreation–tourism sector, *Mitig. Adapt. Strat. Gl.*, 13, 577–596, <https://doi.org/10.1007/s11027-007-9136-z>, 2008.
- Sturm, M.: White water: Fifty years of snow research in WRR and the outlook for the future, *Water Resour. Res.*, 51, 4948–4965, <https://doi.org/10.1002/2015WR017242>, 2015.
- Sturm, M. and Holmgren, J.: An automatic snow depth probe for field validation campaigns, *Water Resour. Res.*, 54, 9695–9701, <https://doi.org/10.1029/2018WR023559>, 2018.
- Sutinen, R., Närhi, P., Middleton, M., Hänninen, P., Timonen, M. and Sutinen, M.L.: Advance of Norway spruce (*Picea abies*) onto mafic Lommelunturi fell in Finnish Lapland during the last 200 years, *Boreas*, 41, 367–378, <https://doi.org/10.1111/j.1502-3885.2011.00238.x>, 2012.
- SYKE: Corine Land Cover 2018, Finnish Environmental Institute [data set], <http://data.europa.eu/88u/dataset/-0b4b2fac-adf1-43a1-a829-70f02bf0c0e5-?locale=en> (last access: 14 October 2019), 2019.
- Vander Jagt, B., Lucieer, A., Wallace, L., Turner, D., and Durand, M.: Snow depth retrieval with UAS using photogrammetric techniques, *Geosciences*, 5, 264–285, <https://doi.org/10.3390/geosciences5030264>, 2015.
- Varhola, A., Coops, N. C., Weiler, M., and Moore, R. D.: Forest canopy effects on snow accumulation and ablation: An integrative review of empirical results, *J. Hydrol.*, 392, 219–233, <https://doi.org/10.1016/j.jhydrol.2010.08.009>, 2010.
- Webster, C., Rutter, N., Zahner, F., and Jonas, T.: Modeling sub-canopy incoming longwave radiation to seasonal snow using air and tree trunk temperatures, *J. Geophys. Res.-Atmos.*, 121, 1220–1235, <https://doi.org/10.1002/2015JD024099>, 2016.
- Zhang, Z., Glaser, S., Bales, R., Conklin, M., Rice, R., and Marks, D.: Insights into mountain precipitation and snowpack from a basin-scale wireless-sensor network, *Water Resour. Res.*, 53, 6626–6641, <https://doi.org/10.1002/2016WR018825>, 2017.